PHILOSOPHICAL TRANSACTIONS OF THE ROYAL SOCIETY A MATHEMATICAL, PHYSICAL & ENGINEERING SCIENCES

State of Stress and Crustal Deformation along Weak Transform Faults

Mark D. Zoback

Phil. Trans. R. Soc. Lond. A 1991 **337**, 141-150
doi: 10.1098/rsta.1991.0112

State of stress and crustal deformation along weak transform faults

By Mark D. Zoback

Department of Geophysics, Stanford University, Stanford, California 94305, U.S.A.

The state of stress and style of crustal deformation along weak transform plate boundaries is discussed in the context of available data and simple analytical models. Appreciable evidence indicates that while the frictional strength of the upper crust is high (in general accordance with simple faulting theory and laboratory-derived coefficients of friction), the frictional resistance to motion along transform plate boundaries is extremely low. These conditions require that horizontal principal stresses must be oriented approximately parallel and perpendicular to the transform-fault zone to minimize the shear stresses acting parallel to the transform. Along plate margins that must accommodate relative convergence (transpressive margins), a pattern of near-fault-normal compression and fault-normal crustal shortening is expected. Along divergent plate margins (transtensional margins), extension is expected to occur perpendicular to the transform, as the direction of minimum horizontal principal stress is expected to be nearly perpendicular to it. These patterns of stress and deformation can be observed along a number of transform faults around the world.

1. Introduction

In situ stress measurements to depths of about 3 km in reverse, strike–slip and normal-fault environments indicate states of stress consistent with Mohr–Coulomb frictional faulting theory and laboratory-derived coefficients of friction (Raleigh *et al.* 1972; McGarr & Gay 1978; Brace & Kohlstedt 1980; Zoback & Hickman 1982; Pine *et al.* 1983; Zoback & Healy 1984; Stock *et al.* 1985; Baumgärtner & Zoback 1989; Baumgärtner *et al.* 1990; Zoback & Healy 1991). These data would seem to argue that it is relatively simple to predict the state of stress in the lithosphere utilizing 'Byerlee's law' (Byerlee 1978) for the brittle upper crust and uppermost mantle and a power-law creep rheology (which is dependent on mineralogy, temperature and strain rate) for the ductily deforming lower crust and deeper mantle (Kirby 1980; Sibson 1982, 1983; Chen & Molnar 1983; Smith & Bruhn 1984; Molnar 1988).

However, in marked contradiction to Byerlee's law, a growing set of data indicates that motion along major plate-bounding transform faults like the San Andreas is resisted by extremely small shear stresses. These data include conductive heat-flow measurements in numerous, relatively shallow boreholes drilled along the length of the San Andreas fault but which detect no evidence of frictionally generated heat (see Brune *et al.* 1969; Henyey & Wasserburg 1971; Lachenbruch & Sass 1973, 1980, 1988). These data imply that the average frictional resistance to fault motion is no greater than about 20 MPa (Lachenbruch & Sass 1981). For the case of hydrostatic pore pressure, Byerlee's law predicts levels of shear stress of about 150 MPa at about 15 km for strike–slip faulting. In addition, data on the orientation of principal

Phil. Trans. R. Soc. Lond. A (1991) **337**, 141–150
Printed in Great Britain

horizontal stresses obtained from earthquake focal-plane mechanisms and borehole measurements in central California show that there is extremely small shear stress acting on planes parallel to the San Andreas fault because the direction of the maximum horizontal principal stress is nearly perpendicular to the strike of the fault (Zoback *et al.* 1987; Mount & Suppe 1987; Oppenheimer *et al.* 1988; Wong 1990). In a 3.5 km deep borehole drilled adjacent to the fault at Cajon Pass, California (a site presumably quite late in the earthquake cycle) a complete lack of right-lateral shear stress on planes parallel to the San Andreas fault was found (Shamir & Zoback 1991; Zoback & Healy 1991) even though the measured differential stress levels were consistent with Byerlee's law. These data indicate that while the frictional strength of faulted crust adjacent to the San Andreas fault is high, the frictional strength of the fault itself is quite low. Also in the Cajon Pass borehole, no evidence was found of fault-generated frictional heat, nor of heat redistribution due to thermal convection (Lachenbruch & Sass 1991), thereby substantiating the validity of the heat-flow measurements in shallow boreholes along the length of the fault. Finally, the near-orthogonal relationship between oceanic transform faults and oceanic spreading centres implies that the resistance to spreading is much greater than that to shear motion along the transforms (Lachenbruch & Thompson 1972; Oldenburg & Brune 1972, 1975). Wilcock *et al.* (1990) have recently shown that normal-faulting microearthquakes adjacent to the Kane transform fault have B and T axes that are approximately parallel and perpendicular to the transform.

2. A conceptual model of stress and deformation along weak transform faults

Taken together, the data referred to above suggest that faulting and crustal deformation along weak transform plate boundaries are controlled by a 'strong crust and weak transform'. Shear stress in the crust appears to be generally high (i.e. consistent with Byerlee's law), whereas shear stresses resolved on planes parallel to the transform faults appear to be quite low. Zoback *et al.* (1987) argued that, if the San Andreas fault was quite weak, principal stresses must be oriented parallel and perpendicular to it so as to result in low shear stress parallel to the transform. The simple cartoon in figure 1 represents the conceptual relationship between stress directions and deformation along a transform plate boundary that is considerably weaker than the adjacent crust. This cartoon is presented in the context of a map based on an oblique Mercator projection about the pole of relative plate motion. With such a projection, a transform fault that exactly coincides with small circles on a globe appear as a straight line parallel to the direction of relative motion. The purpose of figure 1 is to illustrate that for the case of a weak transform fault along a transpressive margin, one would expect a pattern of near-fault-normal compression and fault-normal crustal shortening. Along a weak divergent transform margin extension is expected to occur perpendicular to the transform and the direction of minimum horizontal principal stress is expected to be nearly perpendicular to it.

Figure 2 presents a map of maximum horizontal stress orientations along the San Andreas fault, Cerro Prieto in northern Mexico and the transform faults that form the boundary between the Pacific and North America plates in the Gulf of California. The map is plotted in an oblique Mercator projection using the pole of relative motion between the Pacific and North America plates after DeMets *et al.* (1990).

PHILOSOPHICAL TRANSACTIONS OF THE ROYAL SOCIETY A MATHEMATICAL, PHYSICAL & ENGINEERING SCIENCES

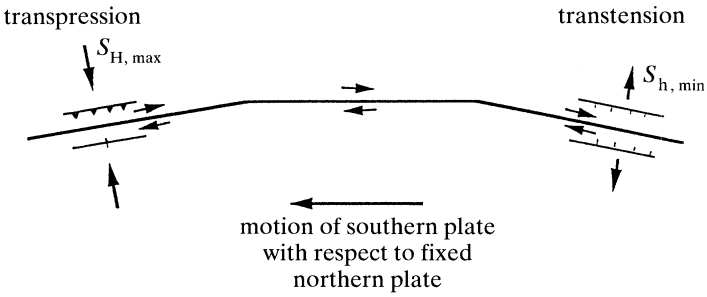

Figure 1. Cartoon illustrating the relationship between the state of stress and deformation along a transform fault that is much weaker than the surrounding crust. For comparison with figure 2, the cartoon is shown in the context of an oblique Mercator projection for the pole of relative motion.

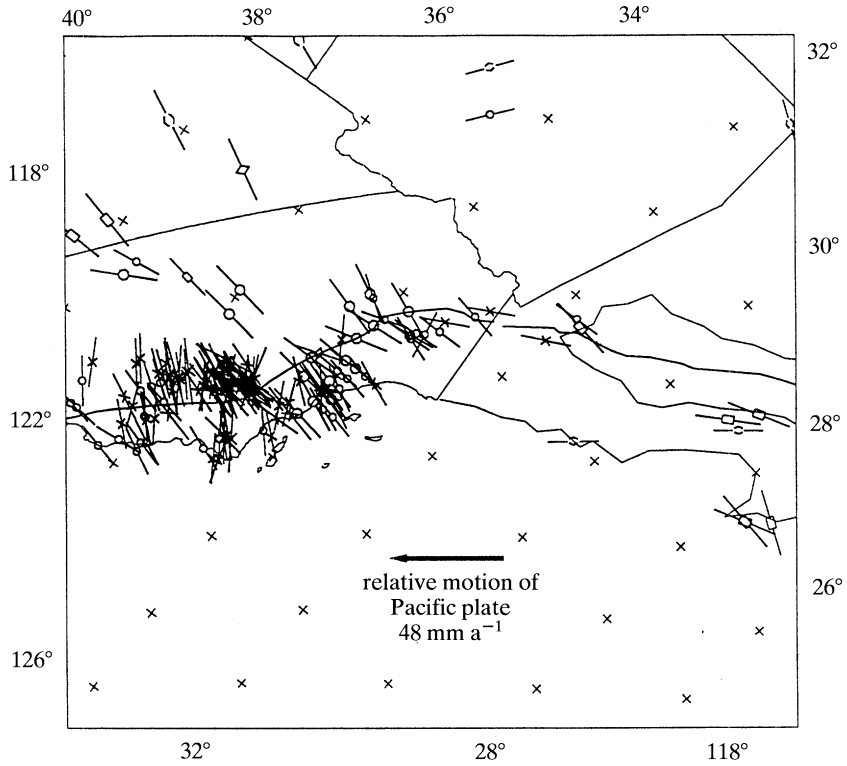

Figure 2. Stress map showing directions of maximum horizontal compression along the San Andreas, Cerro Prieto and Gulf of California transform faults. Map projected about the pole of relative motion between the Pacific and North America plates as given by DeMets *et al.* (1990). The symbol at the centre of each stress orientation indicates the type of stress indicator (circle, earthquake focal plane mechanism; arrow heads, wellbore breakouts; diamond, *in situ* stress measurement; square, geological indicator).

Because the data density is so high in central California only A and B quality data are shown on this map (see Zoback & Zoback 1989).

The manner in which the overall pattern of stress orientation and crustal deformation changes with the trend of the transform is remarkably consistent with the predictions of the simple cartoon shown in figure 1. Near-fault-normal

compression is observed to the north of the eastern Transverse ranges in southern California where the plate motion is relatively convergent, and numerous active folds and reverse faults in the Coast Ranges that trend sub-parallel to the San Andreas fault (Page 1981) clearly indicate fault-normal crustal shortening as indicated in figure 1. Near fault-normal extension (which is shown in figure 2 as near-fault-parallel compression) is observed along southernmost San Andreas fault (near the Salton Sea and Imperial Valley), and along the Cerro Prieto fault and the transform faults in the Gulf of California. Similarly, along the Dead Sea transform in Israel the direction of minimum principal stress is sub-perpendicular to the strike of the fault and near-fault-normal extension is occurring (Eyal & Reches 1983; Letouzey 1986).

Note that transpression or transtension along a weak transform margin need not be constant through time as relative plate motion can change. Although relative plate motion along most of the San Andreas fault is currently convergent, from the late Miocene to Pliocene, tectonism adjacent to the fault was dominated by basin formation and transform-normal extension. About 4 Ma ago, the modern compressional deformation (the onset of folding and reverse faulting indicating shortening perpendicular to the San Andreas fault) coincided with a change in absolute motion of the Pacific Plate (Page & Engebretsen 1984). This change in plate motion resulted in relative-motion vectors changing from slightly divergent to slightly convergent. Similarly, along the Dead Sea transform Eyal & Reches (1983) and Letouzey (1986) discuss a transition from fault-normal compression observed before 8 Ma to the fault-normal extension observed today in the context of a change in relative plate motion.

3. Simple models of the state of stress along weak transform faults

Zoback and others (1987) presented a simple analysis of a weak strike–slip fault based on the assumption that the San Andreas fault zone represents a 'weak fault in a strong crust' and computed the orientation of the maximum principal stress near the fault as a function of the far-field stress orientation and average fault strength. They assumed that the magnitude of the far-field shear stress at depth could be computed from Byerlee's law and that the mean stress magnitude in the crust did not change as a function of distance from the fault. Figure 3 presents an extension of their analysis. Note that, except for the case where the far-field stress orientation is exactly 45° to the fault, a marked change of maximum principal stress direction occurs so as to minimize shear stress parallel to the weak transform. The sense of stress rotation (resulting in either fault-normal compression or fault-normal extension) depends on whether the far-field stress orientation corresponds to either convergent or divergent plate motion. The difference between the near-field and far-field angles depends only weakly on the average strength of the fault as long as it is considerably less than that of the crust far from the fault. As mentioned above an upper bound of 20 MPa for the average frictional strength of the fault is based on the absence of any detectable frictionally generated heat.

Although the calculations shown in figure 3 are based on an extremely simple model, they provide a conceptual framework for interpreting changes from convergent to divergent motion along the strike of a major transform (as illustrated in figure 1) and changes from transpressive to transtensional deformation through time in response to changes of relative plate motion such as observed above for both the San Andreas and Dead Sea transforms.

PHILOSOPHICAL TRANSACTIONS OF THE ROYAL SOCIETY A MATHEMATICAL, PHYSICAL & ENGINEERING SCIENCES

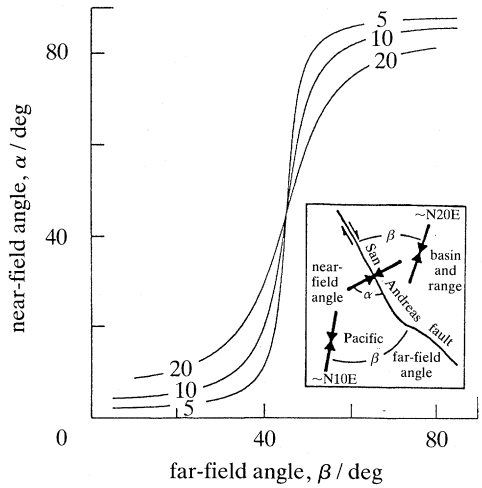

Figure 3. Orientation of maximum horizontal compression near a weak transform fault as a function of the far-field angle for different values of average fault strength (shown in megapascals).

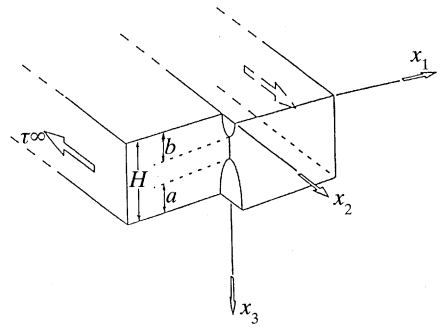

Figure 4. Model of strike–slip plate boundary after Tse *et al.* (1985) in which fault motion is driven by far-field shear τ^∞ and occurs without frictional resistance over the depth ranges indicated by parameters a and b.

To improve upon the simple model of faulting along a weak transform described above, we consider now the state of stress in the vicinity of an extremely weak transform fault by adapting a model derived by Tse *et al.* (1985) that is illustrated in figure 4. In this model motion on a vertical transform fault is driven with a far-field shear stress, τ^∞. The angle between the strike of the fault and the far-field maximum horizontal principal stress is defined by the angle β. There is no frictional resistance to motion over depths defined by the parameters a or b, as defined in the figure. In the calculations below we have chosen $H = 100$ km to correspond to the lithosphere and we assume that there is no frictional resistance to sliding along the 'weak' transform throughout the entire crust and upper mantle. We thus set $b = 50$ km and assume that $a = 0$ because we assume that at depths greater than 50 km both the fault and adjacent lithosphere have the same low strength (see below).

For the parameters defined above, figure 5*a* shows the calculated orientation of $S_{\mathrm{H,\,max}}$ at different depths in the upper crust for the case when relative plate motion is convergent (i.e. $\beta = 55°$). Fault normal compression is observed directly at the

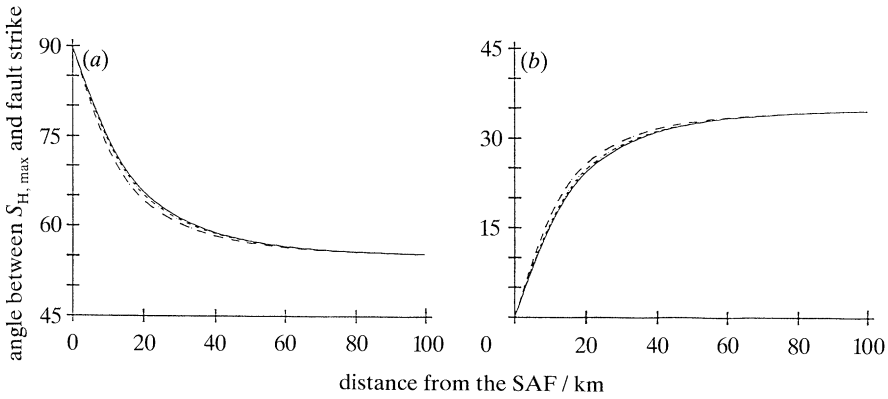

Figure 5. (*a*) Direction of maximum horizontal stress as a function of distance from the San Andreas fault (SAF) for different depths in the crust for the case of a convergent plate margin ($\beta = 55°$, $b = 50$ km). (*b*) Direction of maximum horizontal stress as a function of distance from the San Andreas fault for different depths in the crust for the case of a divergent plate margin ($\beta = 35°$, $b = 50$ km). (*a*, *b*) ——, $z = 3$ km; —·—·—, $z = 9$ km; – – –, $z = 15$ km.

fault (because it has zero frictional resistance) and the $S_{H,max}$ direction gradually approaches the far-field value over a distance comparable to b. The calculated $S_{H,max}$ direction is uniform throughout the upper crust. The case of divergent plate motion is shown in figure 5*b* (for $\beta = 35°$) where it is observed that the direction of maximum horizontal stress is subparallel to the fault at small distances and approaches the far-field stress orientation at distances comparable to b.

It is clear that although the simple model illustrated in figure 4 predicts fault-normal compression (or extension) near the fault, the change in stress orientation with distance is much more continuous and gradual than the broad (*ca.* 100 km) zone of near-fault-normal compression observed adjacent to the San Andreas fault (see Zoback *et al.* 1987). In a strict sense, the only way to explain this, in the context of the model shown in figure 4, would be to make the depth to which the weak fault extended much greater. A reasonable alternative to this hypothesis, however, is simply to consider the San Andreas fault system to be composed of a number of subparallel weak transform faults. Seismicity data clearly define such a series of faults throughout the Coast Ranges (see Hill *et al.* 1990).

4. Crustal decoupling

As originally pointed out by Lachenbruch & Sass (1973), equilibrium conditions require that the lack of frictional resistance along a vertical strike–slip fault be compensated by resistive basal stresses acting on subhorizontal planes adjacent to the fault. For the same model used for the calculations in figure 5*a*, the magnitudes of these drag forces are shown as a function of distance from the fault for different crustal depths in figure 6*a*. As indicated by the left ordinate of figure 6*a*, the calculations are presented as the basal shear normalized by τ^{∞}, the average far-field shear stress. It is clear that potentially large, resistive basal stresses are concentrated in the lower crust within distances to the fault comparable with b.

To compute the absolute magnitude of these resistive basal stresses it is necessary to estimate τ^{∞}. We thus require a far-field constitutive model for the crust and upper mantle along a strike–slip plate margin. We follow Kirby (1980), Sibson (1982, 1983) and others (see §1) and assume that the state of stress is controlled by Byerlee's law

PHILOSOPHICAL TRANSACTIONS OF THE ROYAL SOCIETY A MATHEMATICAL, PHYSICAL & ENGINEERING SCIENCES

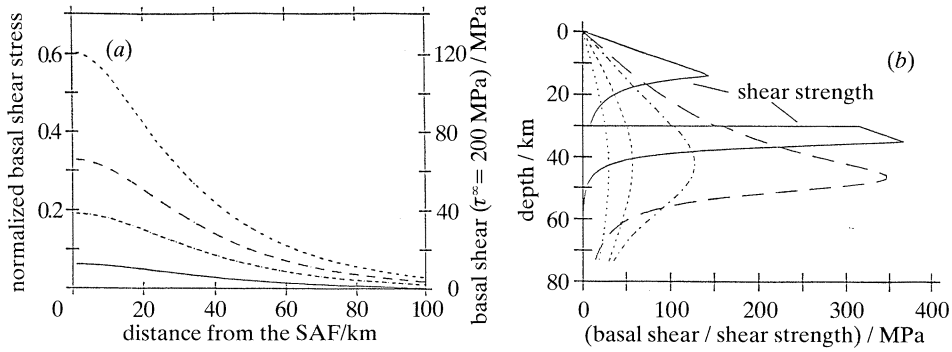

Figure 6. (*a*) Magnitude of resistive basal shear as a function of distance from the San Andreas fault for different depths in the crust. Left ordinate indicates magnitude of basal shear normalized by far-field driving shear stress, τ^∞. Right ordinate indicates magnitude of basal shear for τ^∞ = 200 MPa. ($\beta = 55°$, $b = 50$ km.) ——, $z = 3$ km; —.—.—, $z = 9$ km; ————, $z = 15$ km; – – – –, $z = 25$ km. (*b*) Magnitude of basal shear (for $\tau^\infty = 200$ MPa) as a function of depth at various distances from the fault and shear strength as a function of depth from figure 7 for a strain rate of 10^{-11} s^{-1} (see text). ——, $y = 5$ km; —.—.—, $y = 20$ km; – – – –, $y = 40$ km; · · · ·, $y = 60$ km.

in the upper crust and uppermost mantle and by power-law creep in the lower crust and deeper mantle (figure 7). To arrive at the thickness-averaged far-field driving stress, τ^∞, we will simply divide the cumulative force required to cause deformation (the integral of the strength envelope) by the total thickness. Although it is quite difficult to attempt to calculate precise estimates of strength, several assumptions can be made which effectively result in a lower-bound strength estimate (choosing not to disregard brittle strength completely by assuming, for example, near-lithostatic pore pressure at depth). By multiplying τ^∞ by the normalized basal shear shown in figure 6*a*, we can then predict a minimum value for the basal shear resistance. The calculations of shear strength shown in figure 7 are done for a representative regional heat flow for western California (Lachenbruch & Sass 1973, 1980), a crustal thickness of 30 km and a mean normal stress acting on the transform fault that is approximately equal to the lithostatic stress (i.e. the far-field vertical stress is assumed to be approximately equal to the mean of the two horizontal principal stresses). Stresses are calculated for strain rates of 10^{-11}, 10^{-12} and 10^{-13} s^{-1}, which encompasses reasonable values for the plate-boundary region. An olivine composition is assumed for the mantle. For a heat flow of 71 mW m^{-2} the mantle has extremely low strength below 50 km, regardless of the strain rate. Two assumptions that are quite important with respect to computing a lower-bound estimate for τ^∞ are 1) a granitic composition for the lower crust (after Sibson 1982, 1983), which promotes creep at relatively shallow depth and 2) that hydrostatic pore pressure exists and that the effective-stress principal governs faulting in the brittle régimes throughout the upper crust and uppermost mantle.

For the assumptions stated above and far-field strain rates between 10^{-13} and 10^{-11} s^{-1}, the cumulative force needed to deform the crust and upper mantle is between about 5×10^{12} and 10^{13} N m^{-1}, corresponding to τ^∞ of 100–200 MPa averaged over a 100 km thick lithosphere. Multiplying this value by the normalized basal shear stress shown by the left ordinate of figure 6*a* yields the estimates of basal shear indicated by the right ordinate of figure 6*a* (the values shown correspond to τ^∞ of 200 MPa). If we had assumed that the composition of the lower crust was more

PHILOSOPHICAL TRANSACTIONS OF THE ROYAL SOCIETY A MATHEMATICAL, PHYSICAL & ENGINEERING SCIENCES

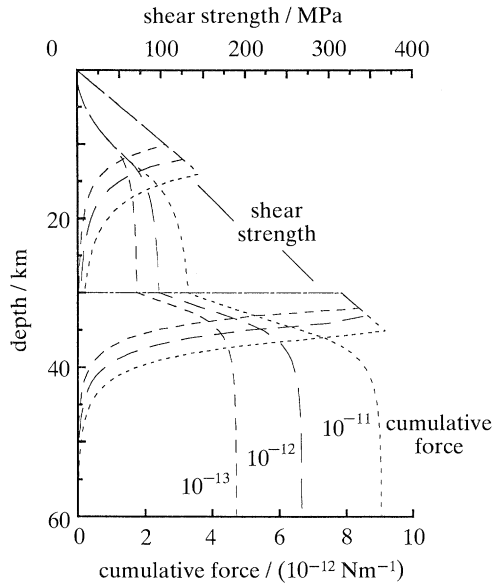

Figure 7. Shear strength and cumulative force as a function of depth and strain rate (s^{-1}) for a strike–slip faulting régime and a heat-flow characteristic of western California. Other parameters and assumptions are explained in the text.

mafic, or if the upper mantle had deformed under effectively 'dry' conditions (either because no pore fluid was present or because the effective stress principal did not apply) a greater cumulative force would have resulted which would cause the basal shear stresses shown in figure 6*a* to be even higher.

An important question about the magnitude of the basal shear stress is whether it is capable of causing faulting along horizontal planes. Because it was assumed that the normal stress on vertical strike–slip faults was approximately equal to the lithostat (figure 7), the strength envelopes used in that figure are also appropriate for a subhorizontal fault plane. In figure 6*b* we overlay the magnitudes of the basal shear at various depths with the strength envelope, for a strain rate of 10^{-11} s^{-1}, that was shown in figure 7. It can be seen that close to the fault the magnitude of basal shear exceeds the strength at depths greater than 15–20 km in the lower crust, and at depths beneath the strong mantle-lid. Thus, as predicted by Lachenbruch & Sass (1973), the motion of the upper crust along weak transforms like the San Andreas fault seems to be resisted by a decoupled lower crust.

References

Baumgärtner, J. & Zoback, M. D. 1989 Interpretation of hydraulic fracturing pressure–time using interactive analysis methods. *Int. J. Rock Mech. Min. Sci.* **26**, 461–470.

Baumgärtner, J., Rummel, F. & Zoback, M. D. 1990 Hydraulic fracturing in situ stress measurements to 3 km depth in the KTB pilot hole VB. A summary of a preliminary data evaluation. In *KTB Rep.* 90–6*a*, 353–400.

Brace, W. F. & Kohlstedt, D. L. 1980 Limits on lithospheric stress imposed by laboratory experiments. *J. geophys. Res.* **85**, 6248–6252.

Brune, J. N., Henyey, T. L. & Roy, R. F. 1969 Heat flow, stress, and rate of slip along the San Andreas fault, California. *J. geophys. Res.* **74**, 3821–3827.

Byerlee, J. D. 1978 Friction of rocks. *Pure appl. Geophys.* **116**, 615–629.

PHILOSOPHICAL TRANSACTIONS OF THE ROYAL SOCIETY A MATHEMATICAL, PHYSICAL & ENGINEERING SCIENCES

Chen, W. P. & Molnar, P. 1983 Focal depths of intracontinental and intraplate earthquakes and their implications for the thermal and mechanical properties of the lithosphere. *J. geophys. Res.* **88**, 4183–4214.

DeMets, D., Gordon, R. G., Argus, D. F. & Stein, S. 1990 Current plate motions. *Geophys. J. Int.* **101**, 425–478.

Eyal, Y. & Reches, Z. 1983 Tectonic analysis of the Dead Sea rift region since the Late-Cretaceous based on megostructures. *Tectonics* **2**, 167–185.

Henyey, T. L. & Wasserburg, G. J. 1971 Heat flow near major strike–slip faults in California. *J. geophys. Res.* **76**, 7924–7946.

Hill, D., Eaton, J. P. & Jones, L. M. 1990 Seismicity, 1980–1986. In *The San Andreas fault system, California* (ed. R. Wallace), pp. 115–152. U.S. Geological Survey Professional Paper 1515.

Kirby, S. 1980 Tectonic stresses in the lithosphere: constraints provided by the experimental deformation of rocks. *J. geophys. Res.* **85**, 6353–6363.

Lachenbruch, A. H. & Sass, J. H. 1973 Thermo-mechanical aspects of the San Andreas fault system. In *Proc. Conf. Tectonic Problems of the San Andreas Fault System* (ed. R. L. Kovach & A. Nur), pp. 192–205. Palo Alto: Stanford University Press.

Lachenbruch, A. H. & Sass, J. H. 1980 Heat flow and energetics of the San Andreas fault zone. *J. geophys. Res.* **85**, 6185–6223.

Lachenbruch, A. H. & Sass, J. H. 1981 Corrections to 'Heat flow and energetics of the San Andreas fault zone' and some additional comments on the relation between fault friction and observed heat flow. *J. geophys. Res.* **86**, 7171–7172.

Lachenbruch, A. H. & Sass, J. H. 1988 The stress heat-flow paradox and preliminary thermal results from Cajon Pass. *Geophys. Res. Lett.* **15**, 981–984.

Lachenbruch, A. H. & Sass, J. H. 1991 Heat flow from Cajon Pass, fault strength and tectonic implications. *J. geophys. Res.* (In the press.)

Lachenbruch, A. H. & Thompson, G. A. 1972 Oceanic ridges and transform faults: their intersection angles and resistance to place motion. *Earth planet. Sci. Lett.* **15**, 116–122.

Letouzey, J. 1986 Cenozoic paleo-stress pattern in the Alpine foreland and structural interpretation in a platform basin. *Tectonophys.* **132**, 215–231.

McGarr, A. & Gay, N. C. 1978 State of stress in the Earth's crust. *A. Rev. Earth planet. Sci.* **6**, 405–436.

Molnar, P. 1988 Continental tectonics in the aftermath of plate tectonics. *Nature, Lond.* **335**, 131–137.

Mount, V. S. & Suppe, J. 1987 State of stress near the San Andreas fault: implications for wrench tectonics. *Geology* **15**, 1143–1146.

Oldenburg, D. W. & Brune, J. 1972 Ridge transform fault spreading pattern in freezing wax. *Science, Wash.* **178**, 301–304.

Oldenburg, D. W. & Brune, J. N. 1975 An explanation for the orthogonality of ocean ridges and transform faults. *J. geophys. Res.* **80**, 2575–2585.

Oppenheimer, D. H., Reasenberg, P. A. & Simpson, R. W. 1988 Fault-plane solutions for the 1984 Morgan Hill, California earthquake sequence: evidence for the state of stress on the Calaveras fault. *J. geophys. Res.* **93**, 9007–9026.

Page, B. 1981 The southern Coast Ranges. In *The geotectonic development of California* (ed. W. G. Ernst). Englewood Cliffs, New Jersey: Prentice-Hall.

Page, B. & Engebretson, D. C. 1984 Correlation between the geologic record and computed plate motions in central California. *Tectonics* **3**, 133–155.

Pine, R. J., Ledingham, P. & Merrifield, C. M. 1983 *In situ* stress measurement in the Carnmenellis granite. II. Hydrofracture tests at Rosemanowes Quarry to depths of 2000 m. *Int. J. Rock Mech. Min. Sci.* **20**, 63–72.

Raleigh, C. B., Healy, J. H. & Bredehoeft, J. D. 1972 Faulting and crustal stress at Rangely, Colorado. In *Flow and fracture of rocks*, pp. 275–284. Geophysical Monograph, vol. 16. American Geophysical Union.

Shamir, G. & Zoback, M. D. 1991 A crustal stress orientation profile to 3.5 km depth near the San Andreas fault at Cajon Pass, California. *J. geophys. Res.* (Submitted.)

PHILOSOPHICAL TRANSACTIONS OF THE ROYAL SOCIETY A MATHEMATICAL, PHYSICAL & ENGINEERING SCIENCES

Sibson, R. H. 1982 Fault zone models, heat flow, and the depth distribution of earthquakes in the continental crust of the United States. *Bull. seismol. Soc. Am.* **72**, 151–163.

Sibson, R. H. 1983 Continental fault structure and the shallow earthquake source. *J. Geol. Soc. Lond.* **140**, 741–767.

Smith, R. B. & Bruhn, R. L. 1984 Intraplate extensional tectonics of the eastern Basin-Range: inferences on structural style from seismic reflection data, regional tectonics, and thermal-mechanical models of brittle–ductile transition. *J. geophys. Res.* **89**, 5733–5762.

Stock, J. M., Healy, J. H., Hickman, S. H. & Zoback, M. D. 1985 Hydraulic fracturing stress measurements at Yucca Mountain, Nevada, and the relationship to the regional stress field. *J. geophys. Res.* **90**, 8691–8706.

Tse, S. T., Dmoska, R. & Rice, J. R. 1985 Stressing of locked patches along a creeping fault. *Bull. seismol. Soc. Am.* **75**, 709–736.

Wilcock, W. S. D., Purdy, G. M. & Solomon, S. C. 1990 Microearthquake evidence for extension across the Kane transform fault. *J. geophys. Res.* **95**, 15439–15462.

Wong, I. 1990 Seismotectonics of the Coast Ranges in the vicinity of Lake Berryessa, northern California. *Bull. seismol. Soc. Am.* **80**, 935–950.

Zoback, M. D. & Healy, J. H. 1984 Friction, faulting and *in situ* stress. *Annls Geophisicae* **2**, 689–698.

Zoback, M. D. & Healy, J. H. 1991 *In situ* stress measurements to 3.5 km depth in the Cajon Pass Scientific Research Borehole: implications for the mechanics of crustal faulting. *J. geophys. Res.* (In the press.)

Zoback, M. D. & Hickman, S. 1982 *In situ* study of the physical mechanisms controlling induced seismicity at Monticello Reservoir, South Carolina. *J. geophys. Res.* **87**, 6959–6974.

Zoback, M. D., Zoback, M. L., Mount, V. S., Suppe, J., Eaton, J. P., Healy, J. H., Oppenheimer, D., Reasenberg, P., Jones, L., Raleigh, C. B., Wong, I. G., Scotti, O. & Wentworth, C. 1987 New evidence on the state of stress of the San Andreas fault system. *Science, Wash.* **238**, 1105–1111.

Zoback, M. L. & Zoback, M. D. 1989 Tectonic stress field of the conterminous United States. *Geol. Soc. Am. Mem.* **172**, 523–539.

PHILOSOPHICAL TRANSACTIONS OF THE ROYAL SOCIETY A MATHEMATICAL, PHYSICAL & ENGINEERING SCIENCES